Atmos. Chem. Phys. Discuss., 11, 8801–8840, 2011
www.atmos-chem-phys-discuss.net/11/8801/2011/
doi:10.5194/acpd-11-8801-2011

Atmospheric Chemistry and Physics Discussions

Cloud condensation nuclei closure study on summer arctic aerosol

M. Martin[1], R. Y.-W. Chang[2], B. Sierau[1], S. Sjogren[3], E. Swietlicki[3], J. P. D. Abbatt[2], C. Leck[4], and U. Lohmann[1]

[1]Institute for Atmospheric and Climate Science, ETH Zurich, Zurich, Switzerland
[2]Department of Chemistry, University of Toronto, Toronto, Canada
[3]Division of Nuclear Physics, Lund University, Lund, Sweden
[4]Department of Meteorology, Stockholm University, Stockholm, Sweden

Received: 20 February 2011 – Accepted: 27 February 2011 – Published: 14 March 2011

Correspondence to: M. Martin (maria.martin@env.ethz.ch)

Published by Copernicus Publications on behalf of the European Geosciences Union.

Abstract

We present an aerosol – cloud condensation nuclei (CCN) closure study on summer high Arctic aerosol based on measurements that were carried out in summer 2008 during the Arctic Summer Cloud Ocean Study (ASCOS) on board the Swedish ice breaker *Oden*. The data presented here were collected during a three-week time period in the pack ice (> 85° N) when the icebreaker *Oden* was moored to an ice floe and drifted passively during the most biological active period into autumn freeze up conditions.

CCN number concentrations were obtained using two CCN counters measuring at different supersaturations. The directly measured CCN number concentration is then compared with a CCN number concentration calculated using both bulk aerosol mass composition data from an aerosol mass spectrometer and aerosol number size distributions obtained from a differential mobility particle sizer, assuming κ-Köhler theory and an internally mixed aerosol.

For the two highest measured supersaturations, 0.73 and 0.41%, closure could not be achieved with the investigated settings concerning hygroscopicity and density. The calculated CCN number concentration was always higher than the measured one. One possible explanation is that the smaller particles that activate at these supersaturations have a relative larger insoluble organic mass fraction and thus are less good CCN than the larger particles. At 0.20, 0.15 and 0.10% supersaturation, the measured CCN number can be represented with different parameters for the hygroscopicity and density of the particles. For the best agreement of the calculated CCN number concentration with the measured one the organic fraction of the aerosol needs to be nearly insoluble ($\kappa_{org} = 0.02$). However, this is not unambigious and $\kappa_{org} = 0.2$ is found as an upper limit at 0.1% supersaturation.

ACPD
11, 8801–8840, 2011

M. Martin et al.

1 Introduction

Aerosol particles in the atmosphere can influence climate in several ways. First, they can directly scatter and absorb radiation (direct aerosol effect). Second, they can act as cloud condensation nuclei (CCN) or ice nuclei and change the properties of clouds, which is called the indirect aerosol effect (see e.g. Lohmann and Feichter, 2005). Both effects are a matter of current research, as aerosol-cloud interaction processes are generally not well understood, and the impact of the various aerosol effects on climate and climate change is still unknown (Denman et al., 2007).

Clouds themselves play a key role in our understanding of the climate system. This is also true for Arctic low level clouds (Walsh et al., 2002; Tjernström et al., 2008). The high Arctic low-level clouds (north of 80° N) have a pronounced influence on the surface energy budget (Sedlar et al., 2010), and thus on the melting and freezing of the perennial sea ice (Kay and Gettelman, 2009). During winter, model experiments indicate that Arctic clouds are optically thicker than elsewhere, predominantly because they tend to include cloud liquid water at much lower temperatures than found elsewhere (e.g. Intrieri et al., 2002; Tjernström et al., 2008). On the opposite, during summer, the high Arctic low-level clouds are optically thin with fewer but larger droplets, which make them reflect shortwave radiation less effectively than clouds with numerous but smaller droplets (e.g. Twomey, 1977).

There is also another difference between summer and winter clouds in the Arctic concerning particle sources. This is caused by the geographical location of the Arctic, which exposes it to an influx of polluted mid-latitude air during November to April, reinforced by photochemical oxidation at polar sunrise. In winter to early spring Arctic aerosol concentrations may reach up to 20 times the pre-industrial levels, a phenomenon referred to as Arctic haze (Heintzenberg and Leck, 1994; Shaw, 1995; Korhonen et al., 2008). In contrast to winter, summer conditions are much more pristine, typically resulting in low and relatively stable aerosol concentrations of approximately 20–60 cm^{-3} in the accumulation mode

(Covert et al., 1996; Bigg et al, 1996; Heintzenberg et al., 2006) over the pack ice area north of 80° N. It is possible that long-range transport of pollutants are also a source then, but during the high Arctic summer: (1) it precipitates more, which lowers aerosol mass and number by scavenging, specifically at the marginal ice zone (Nilsson and Leck, 2002; Heintzenberg et al., 2006); (2) air masses tend to be transported from cleaner regions (Stohl et al., 2006); and (3) during a former campaign it was observed that Aitken mode concentrations are higher than accumulation mode concentrations, which is opposite to winter-time observations (Heintzenberg et al., 2006). All of these findings suggest that the major source of particles in summer is different from that in winter.

Marine biology is proposed to be a source of Arctic summertime CCN (see e.g. Li and Barrie, 1993; Heintzenberg and Leck, 1994; Leck and Persson, 1996; Quinn et al., 2002; Leck and Bigg, 2005a). This source is expected to be more active in summer, as ice melts and more solar radiation reaches the ocean, which leads to increased biological activity. Dimethyl sulphide (DMS), a gas produced by marine organisms, is thought to be a good precursor for CCN (Charlson et al. (1987)). It mainly oxidizes photochemically to sulfur dioxide (SO_2), which reacts in the atmosphere and/or within cloud droplets to form sulfuric acid (H_2SO_4). Gas-phase H_2SO_4 is then the suggested precursor for aerosol nucleation, but it also condenses on pre-existing particles. Although the major source region of the aerosol precursor gas, DMS, was confined to the biological open waters at the ice edge, the at least 2–3 days residence time of DMS in air enabled it to be advected over the pack ice area and support it with major CCN precursor-components through its photochemical oxidation (Leck and Persson, 1996). Furthermore, from research carried out during three ice-breaker expeditions in the summers of 1991, 1996 and 2001 (Leck et al., 1996, 2001, 2004) a new picture of aerosol properties with implication for CCN activation has been suggested (Leck and Bigg, 2005b): DMS concentration would determine the mass of sulfate by producing material for growth of the particles, but would have only a minor influence on the number of CCN forming the low-level clouds. Instead the number of airborne microcolloids

ACPD
11, 8801–8840, 2011

and their gels, called exopolymer secretions (EPS) or microgels, emitted from the surface microlayer of the open leads through bubble bursting mechanisms has been put forward for consideration to mainly contribute to the number of cloud drops over the pack ice area. However, the hygroscopic properties, the cloud nucleating ability of these biogenic particles, and their source and sink strengths are still not well understood.

So far, CCN measurements over the high Arctic pack ice area in summer are few due to its remoteness. Bigg and Leck (2001) report daily mean CCN number concentrations of 15 to 50 cm^{-3} at 0.25% supersaturation, with a variability over three orders of magnitude within a day, although concentrations were usually lower than 100 cm^{-3}, occasionally less than 1 cm^{-3} (e.g. Lannefors et al., 1983; Bigg et al., 2001; Leck et al., 2002; Mauritsen et al., 2011). Mauritsen et al. (2011) summarize frequency distributions of observed CCN number concentrations from four high Arctic expeditions (including the most recent data set collected during ASCOS (Arctic Summer Cloud Ocean Study) in the summer of 2008) measured at different supersaturations (ranging from 0.1 to 0.8 %). All four populations showed an overall consistent distribution with three quarters of the CCN number concentrations being greater than 10 cm^{-3} but less than about 100 cm^{-3}, medians typically in the range of 15 to 50 cm^{-3}. Bigg and Leck (2001) performed a closure study by calculating a predicted CCN number concentration from size distribution data and assuming that the particles consist only of ammonium sulfate. This gave them a good correlation with the measured CCN data, but an overprediction (more CCN were calculated than measured) of around 30% was determined. To investigate the role of chemistry in more detail, Zhou et al. (2001) performed a closure study using additional hygroscopic growth information and an indirect measure on chemistry, and assuming that the calculated CCN particles were composed of ammonium sulfate, a nearly insoluble fraction and sodium chloride. These assumptions yielded a similar overprediction as found by Bigg and Leck (2001), and the reason remained unclear. Furthermore, Leck et al. (2002) used direct measure of chemical composition, state of mixture and morphology to discuss sources and methods of production of CCN.

ACPD
11, 8801–8840, 2011

Measured CCN concentrations were on average less than would have been expected from either a sulfate or a sea-salt composition and the observed particle-number size distribution. It was concluded that other components, probably organics, depressed the nucleating ability of the particles.

In this paper, we present an aerosol-CCN closure study on data taken during a campaign in the high Arctic on board the Swedish ice breaker *Oden* in summer 2008. The study focuses on a three-week period, where the ship was drifting passively moored to an ice floe at a latitude >87° N, thus during the most biological active period into autumn freeze up conditions. Closure was achieved by comparing measured CCN number concentrations with CCN number concentrations calculated from combined mass spectrometer chemical mass and particle number size distribution data, using κ-Köhler theory (Petters and Kreidenweis, 2007). Conclusions can then be drawn on the assumptions made (e.g. concerning the hygroscopicity of the particles and their components) based on the outcome of the closure.

2 Cruise details

The ASCOS campaign was carried out on the Swedish ice breaker *Oden*. The cruise started on 2 August 2008 (DoY 215) in Longyearbyen, Svalbard. Figure 1 shows the ship track of the cruise. First, the ship headed westwards into the Greenland Sea Fram Strait area where it stopped for an open water station on 3 August (DoY 216). After that, the cruise was continued northwards through the marginal ice zone, where measurements were taken from 4 August (DoY 217) to 5 August (DoY 218). From there, *Oden* went north through the pack ice until it was docked on the ice floe at around 87° N on 12 August (DoY 225), 12:00. Then the ship drifted with the ice floe for three weeks until 2 September (DoY 246), 00:10, reaching a latitude of 87°30′ N. From there, *Oden* returned to Longyearbyen on 9 September (DoY 254). On the way back, an additional marginal ice zone station (6 September (DoY 251) to 7 September) and

ACPD
11, 8801–8840, 2011
CCN Closure on Arctic Aerosol
M. Martin et al.

an open water station (7 September (DoY 252)) were conducted. For further cruise details see Paatero et al. (2009). The study presented here uses only data that was collected during the ice drift period.

3 Instrumentation

3.1 Inlet system

An identical sampling manifold was utilized in all four expeditions mentioned in the introduction upstream of all aerosol measurements. Leck et al. (2001) reported further details. In short, the inlet system consisted of two masts which were equipped with a horizontally oriented commercial PM 1 and PM_{10}-inlet, respectively. The PM 1-inlet mast was also used for the gas-phase sampling lines. The inlets were located approximately 25 m above sea level as on previous cruises. The air was drawn in via pipes of the two-masted inlet system that extended at an angle of 45° to about 3 m above the roof of the container. All aerosol instruments used for this study were located in the same container on the foredeck of the ship and sampled from the same PM10 inlet through the main pipe that had an inner diameter of 9 cm and was pumped with a total flow of approx. 1140 l min^{-1}. Only the CCN counter measuring at a constant supersaturation (see below) sampled from the PM1 inlet during certain time periods. The individual particle instruments were served by two distribution lines of 3/8 inch stainless steel tubing that were branched off the main pipe. Aerosol samples were taken isokinetically from the main flow using forward pointing inlets located in the center of the main pipe and connected to the two distribution lines. For each of these inlets and distribution lines, a constant volume flow was generated both from the instruments and a variable back-up flow leading to a total of 16.7 l min^{-1}. With the inlets facing forward and by positioning the ship facing into the wind, local ship pollution could be avoided most of the time. Additionally, direct contamination from the ship was excluded by using a pollution controller. When either sudden high particle number concentrations were

ACPD
11, 8801–8840, 2011

detected by an ultrafine particle counter (UCPC; TSI model 3025; TSI Inc., MN, USA) located upstream of the flow splits to the counters and/or the wind was outside ±70° of the direction of the bow and weaker than $2\,m\,s^{-1}$, the main pumps were turned off and pollution could not reach the sample inlets.

The CCN counters were also connected to the main pipe via one of the distribution lines. The connection had a length of 103 cm plus an additional 105 cm of conductive tubing (6 mm outer diameter) that was branched off the steel tube using a tee. The minor flow split was shared by the two CCN counters and a Condensation Particle Counter (CPC). Each of the CCN counters had a sample flow of $0.5\,l\,min^{-1}$, and the CPC had an additional flow of $0.9\,l\,min^{-1}$. The RH of the sample flow was assumed to be less than 30% based on the residence time of the air inside the flow system and the temperature difference between ambient and laboratory temperature.

Diffusional losses of particles inside the tubing section from the isokinetic inlet of the distribution line to the CCNCs were calculated to be in the range of 5% for a 30 nm diamter particle. As diffusional losses decrease with increasing particle size, these losses were neglected and not corrected for herein.

Gravitational losses of particles > 1 µm diameter have been neglected in our considerations as particles of this size have been barely observed during the cruise. Gravitational settling of 1 µm diameter particles would account for approx. 1% loss in a 90° bend section (assuming the flow conditions for the distribution-lines described above), and for less than 1% in the straight tube sections from the isokinetic sampling manifold to the CCN-tee. The flow system included five 90° bend sections.

3.2 CCN counters

The instrument used to measure the CCN number concentration was a continuous-flow streamwise thermal gradient CCN counter (CCNC). It is built and distributed by Droplet Measurement Technologies (DMT, Boulder USA), and used by several research groups worldwide. Its working principle is described in full detail by Roberts and Nenes (2005).

The main part of the instrument is a cylindrical, upright standing column. An inside

ACPD
11, 8801–8840, 2011

temperature gradient is established, with the lowest temperature at the top. The walls of this column are wetted with water. Thus, heat and water vapour are transported towards the center of the column by diffusion. As heat diffuses more slowly than water in air in the temperature range used, a constant supersaturation (SS) is established in the center of the column. This supersaturation can be adjusted by changing the temperature gradient of the column.

Aerosol particles enter the instrument through an inlet at the top and pass through the column where they can activate and grow to droplet size. At the outlet of the column the activated particles are counted with an optical particle counter (OPC), which counts all particles bigger than 1 µm in diameter as cloud condensation nuclei. The CCNC undercounts particles, when they are not growing larger than 1 µm until they reach the OPC. However, in the study presented here, most particles were found in size bins larger than 1 µm, and were thus counted correctly as CCN.

The temperature determining the supersaturation of the instrument was calibrated several times during the cruise for both counters using monodisperse ammonium sulfate particles, which have a known activation curve. The particles are first size-selected using a differential mobility analyzer, and then passed through the DMT CCNC. As the particle size increases, the activated fraction increases. From a certain size onwards, all particles activate. The dry activation diameter (D_d) is defined as the size at which 50 % of the particles activate, and can be determined by fitting the activated fraction versus the dry particle size. The critical supersaturation S_{crit} can then be calculated using Köhler theory. It is used as a calibration value for the measured SS. A detailed description on calibrating the DMT CCNC can be found in Rose et al. (2008).

During this study, two CCN counters were operated in parallel. The first counter (counter 1) scanned five different SS with a measurement period of 30 mi each. The settings of this counter were adjusted after each calibration, i.e. several times during the cruise. Thus, the supersaturations at which CCN properties are presented herein varies for different time periods. Difficulties in calibrating the CCN counters were encountered on board the ship that led to a relatively large uncertainty in the supersaturations of 6–10%. The difficulties were mainly due to problems with the particle generation system. Furthermore, the flow ratio of the sheath to the sample flow was around 1:13 instead of the ideal 1:10 because of problems caused by the flow measurement. The second CCN counter (counter 2) was set to a constant supersaturation, which was slightly increased once for better comparison with CCN data collected during three former expeditions. The values of the supersaturations of both counters are summarized in Table 1. The two counters compare very well, although their exact supersaturation differs. This is shown in more detail in Sect. 5. The instruments were deployed in parallel with a Condensation Particle Counter (CPC 3785, TSI Inc., USA), which measured the total number of aerosols larger than 5 nm in diameter.

3.3 Aerosol mass spectrometer

A unit-mass resolution time-of-flight (C-ToF) aerosol mass spectrometer (AMS, Aerodyne Research Incorporated, Billerica, USA) sampled ambient particles from 70 nm to 500 nm diameter with near 100% efficiency. Particles were vapourised and ionised (70 eV) in a vacuum chamber and the resulting species were detected with a time-of-flight mass spectrometer. The detected signal was attributed to sulphate, nitrate, organics and methane sulphonate that was non-refractory at 10^{-7} torr and 873 K, in order to determine the particle chemical composition. This study makes use of the bulk aerosol chemical composition which was averaged over a sampling time of 5 min. Further details on the instrument's general operation can be found in the literature (Canagaratna et al. (2007); Drewnick et al. (2005); Jimenez et al. (2003)), and the specific details for this study can be found in Chang et al. (2010). Although cascade impactor measurements with 6–24 h time resolution on aerosol chemical composition resolved over size were also available, the AMS data were chosen for this analysis due to its relatively higher time resolution.

ACPD
11, 8801–8840, 2011

3.4 Tandem differential mobility particle sizer

To measure the particle number size distribution one large and one small Hauke-type differential mobility analyzer were run in tandem (TDMPS) to cover the mobility size range 3–800 nm in diameter. The small DMA was set to a sample:sheath air flow ratio of 02:20, the large DMA to a ratio of 1:5, with a total flowrate of 3 l min^{-1}. Three mobility channels overlapped between the two DMAs to give a continuous number size distribution (Birmili et al., 1999).

The CPC on the same flow split as the CCN counters measured on average 20% less than the DMPS system, when integrating the DMPS data from the cut-off of the CCNC-CPC. One part of this difference can be explained by particle losses due to diffusion as the CPC was located further down the line than the DMPS. These losses accounted for ≈ 5% (calculated for 30 nm diameter particles), but cannot explain the difference of 20%. As the cut-off of the CCNC-CPC was not calibrated, the integrated number concentration of the quality assured DMPS system was finally used for the data and error analysis presented herein. The DMPS measurements agreed well with measurements from another DMPS system on board the ship.

3.5 Error analysis

The uncertainty of the CCNC measurements is mainly due to the uncertainty of the set supersaturation, which was calibrated several times. These calibrations showed a uncertainty of 5–10% depending on the supersaturations (see Table 1 for exact values). The calculated uncertainty of the DMPS system was based on taking Poisson statistics for the measured number concentrations. Uncertainties in the measured AMS mass at each mass-to-charge ratio were estimated from the electronic noise and Poisson statistics for the ion signal. The uncertainty for each species was then determined by adding in quadrature the uncertainty in its component mass-to-charge ratios.

In terms of intercomparison and the total CCN number concentration there is also an error due to diffusion losses in the inlet tubing of the instruments. The three instruments

ACPD
11, 8801–8840, 2011

were located at different spots in the aerosol container connected to the main inlet using different tubing diameters and lengths. Therefore, this error is size-dependent. It was determined to be ≈5 % for 30 nm diameter particles from the main inlet to the CCN counters. The error decreases with increasing size, as diffusion losses become smaller.

4 Analysis

4.1 Theory

Köhler theory describes the relationship between chemical composition, size and supersaturation present at the surface of the droplet in thermodynamic equilibrium. The theory takes into consideration different fundamental properties of a particle, such as surface tension and density. Using this theory, the droplet size of a growing CCN particle can be calculated at a certain SS assuming thermodynamic equilibrium with the environment of the droplet. Köhler theory also provides the critical supersaturation (S_{crit}) that must be overcome before a particle of a certain dry size can activate (e.g. Seinfeld and Pandis, 1998). When keeping all other parameters constant, the larger the particle diameter is, the lower critical supersaturation is required for activation.

The supersaturation (SS) can be written, depending on the water activity a_w, as follows:

$$SS = a_w \exp\left(\frac{4\sigma_{s/a} M_w}{RT\rho_w D}\right), \qquad (1)$$

where $\sigma_{s/a}$ is the surface tension between the solution and air, ρ_w the density of water, M_w its molecular weight, R the universal gas constant, T the absolute temperature, D the diameter of the droplet at the supersaturation SS, and a_w is the activity of water.

ACPD
11, 8801–8840, 2011

This formula can be reformulated using the hygroscopicity parameter κ, as defined by Petters and Kreidenweis (2007), leading to:

$$SS = \frac{D^3 - D_d^3}{D^3 - D_d^3(1-\kappa)} \exp\left(\frac{4\sigma_{s/a} M_w}{RT\rho_w D}\right), \tag{2}$$

where D_d is the volume equivalent diameter of the dry particle. κ depends on the water activity of the particle and the volumes of the dry particle and of the aerosol. It ranges between 0 for insoluble particles, and values >1 for some salts (1.28 for NaCl). κ of a particle is defined as the sum of the products of the κ values of all single solute components i in the particle and their corresponding volume fractions $\epsilon_i = \frac{V_i}{V_{tot}}$:

$$\kappa_{tot} = \sum_i \epsilon_i \kappa_i. \tag{3}$$

4.2 Estimation of CCN number concentrations/closure study

To predict the number of CCN, first κ_{tot} (Eq. 3) needs to be calculated. Therefore, κ values and densities for the separate mass components measured by the AMS have to be assumed. As organic and sulfate were the two most abundant species measured by the AMS (on average 36% and 52% of the total mass, respectively), only those two were considered for this closure analysis. For each mass component one κ value and one density was chosen. As the AMS measures the bulk chemical composition, all particles are assumed to be internally mixed. The hygroscopic measurements from a Hygroscopicity Tandem Differntial Mobility Analyzer (HTDMA), that were also carried out on board, supports an internal mixture over the size range investigated with a

ACPD
11, 8801–8840, 2011

slightly decreasing hygroscopicity with decreasing size. Furthermore, Kammermann et al. (2010) showed in a study from the sub-Arctic region that their CCN predictions were not weakend by assuming an internally mixed aerosol compared to an external mixture.

Next, the supersaturation set in the CCNCs at a given time is taken as the critical supersaturation S_{crit}. With these two parameters, the Köhler equation can be solved analytically for the dry activation diameter D_d.

The number of predicted CCN, CCN_{pred}, can now be calculated from the DMPS size distribution data, assuming that all particles with a diameter larger than D_d act as CCN. In an ideal case, i.e. if the assumptions concerning hygroscopicity, density and the internal mixture of the aerosol are correct, CCN_{pred} should be equal to the measured number of CCN, CCN_{meas}.

For each SS, the parameters κ_{org}, κ_{sulf}, ρ_{org} with the addition of an assumed insoluble fraction of the organic compound (see Table 2) were permuted for sensitivity tests and a more statistical approach. This led to a total set of 90 calculations per supersaturation, thus 450 settings in total for counter 1. For each set, CCN_{pred} was calculated and the slope of the fit of CCN_{pred} vs. CCN_{meas} was determined. κ_{org} was varied assuming organic substances with very different hygroscopicities. We used $\kappa_{org} = 0$ for completely insoluble organic compounds, $\kappa_{org} = 0.1$ and 0.2 (κ_{org} assumed for most lab-produced secondary organic aerosol (Andreae and Rosenfeld, 2008, and references therein)) and $\kappa_{org} = 0.3$ and 0.4 for even more hygroscopic organic fractions. Additionally, the density of the organic substances, ρ_{org}, was varied between 1 g cm^{-3}, 1.2 g cm^{-3} and 1.6 g cm^{-3}. κ_{sulf} for the sulfate particles was changed between 0.7, 0.65 and 0.61, which are values for different typical sulfate compounds. Petters and Kreidenweis (2007) list as CCN derived $\kappa_{sulf} = 0.61$ for $(NH_4)_2SO_4$, $\kappa_{sulf} = 0.65$ for $(NH_4)_3H(SO_4)_2$, and $\kappa_{sulf} = 0.7$ was taken as a mean value for H_2SO_4. Moreover, it was assumed that 0% or 20% of the organic substance is insoluble with a density ρ_{ins} of 1 g cm^{-3}. All permutations are listed in the Appendix in Table 6. Surface tension of water (0.072 N m^{-1} at the given temperature in the laboratory) was assumed for all calculations.

Discussion Paper | Discussion Paper | Discussion Paper | Discussion Paper |

ACPD

11, 8801–8840, 2011

For the closure study presented herein, CCNC, DMPS and AMS data are averaged over 10 min. Data points were only considered, when there was full coverage over 10 min for all three instruments.

5 Results and discussion

Figure 2 exemplarily shows the results of a closure calculation for CCN counter 1 (scanning through five supersaturations). Herein, we assumed a κ_{org} value of 0.3, a density of the organic compound of $\rho_{org} = 1\,g\,cm^{-3}$, κ_{sulf} of 0.65, and a density of $\rho_{sulf} = 1.77\,g\,cm^{-3}$. No insoluble organic fraction was assumed. For this setting, the calculated CCN number concentration is overpredicted (higher number concentration than the measured one) for all five supersaturations, mostly for the two highest supersaturations of 0.41% and 0.73%.

In the whole study, fitting of CCN_{pred} vs CCN_{meas} was done using a least trimmed squares (LTS) fit, introduced by Rousseeuw (1984). This is a robust fitting method using a least square method (for more details see Rousseeuw and van Driessen, 2006 and Muhlbauer et al., 2009). This method also identifies outliers, which are excluded from the fit. These outliers can then be investigated and interpreted separately. Here, the slope and R^2 of the LTS fit for 0.1% SS was 1.29 and 0.98, respectively, and for 0.7% SS it was 1.51 and 0.99, respectively.

To constrain the best estimate for the four investigated parameters for all five supersaturations, permutation runs as described in Sect. 4.2 were performed. In Fig. 3, the results are shown for each individual supersaturation with the different assumptions listed in Table 2. The number of predicted CCN increases mainly with increasing κ_{org}, as it has the largest range of the four varied parameters. As the criterion for achieving closure we took the slope being 1 within the errorbars. The latter were derived from error propagation from the uncertainties described in Sect. 3.5 and then fitting CCN_{pred} vs. CCN_{meas} by adding and subtracting the absolute errors from the found values. The

ACPD
11, 8801–8840, 2011

largest variation from the fit without errors was taken as the uncertainty. R^2 was always >0.97 for all runs and thus not very variable. Based on the above mentioned criterion, closure could be achieved for different settings assuming $\kappa_{org} = 0$, 0.1 or 0.2 for some calculations at 0.10% SS (namely settings 1–6, 9–12, 15–18, 19–23, 25–37, 39, 43–45, 47, 49–53; which are defined in the Appendix Table). For 0.15% and 0.20% SS, closure could only be achieved with $\kappa_{org} = 0$ with setting 13 for both SS and with setting 14 only for 0.15% SS.

The number of outliers given by the LTS fit can also indicate the quality of the fit. At 0.1% SS, the number of outliers is smallest for the lowest run numbers, thus also suggesting a low κ_{org}, while for the higher supersaturations, it does not change significantly between the permutations. The fewest outliers for 0.1% SS was found for permutation 6 ($\kappa_{org} = 0$, $\rho_{org} = 1.6\,\mathrm{g\,cm^{-3}}$, $\kappa_{sulf} = 0.7$).

For the two highest measured supersaturations, 0.41% and 0.73% SS, calculations overpredicted the CCN number for all applied permutations. This might be explained by the fact that the lower cut-off of the AMS measurements is 70 nm, but smaller particles can still act as CCN at these supersaturations. This induces an uncertainty associated with the actual mass concentrations used to calculate κ, as the ratio of the masses might be different for smaller sizes. As closure cannot be achieved with any of the permutations (even when a 20% insoluble organic fraction is assumed), these results suggest that the chemical composition was different for smaller particles. They need to have a larger organic fraction to achieve closure. To account for the case in which a non-hygroscopic component of the aerosol was present but not measured by the AMS, further testing was done by adding a non-hygroscopic organic mass with a density of $1\,\mathrm{g\,cm^{-3}}$ to the total mass. However, closure could only be achieved for 0.71% SS when this insoluble mass was 4 to 5 times higher than the actual measured organic mass. Based on comparisons of mass measured by the AMS and DMPS, it is unlikely that there was this much mass not measured by the AMS for particles >100nm in diameter. However, for Aitken mode particles or smaller, this would be possible within the measurement uncertainties. It should also be mentioned that at smaller sizes the

ACPD
11, 8801–8840, 2011

systematic errors increase (e.g. the AMS composition accuracy, more particle losses), thus, these results at the two highest SS can also be caused – at least partly – by these errors.

The best result for the three lowest supersaturations (0.10%, 0.15%, and 0.20%), when taking the smallest summed difference from each fitted slope to 1 as criteria, was achieved for setting 13 with $\kappa_{org} = 0, \kappa_{sulf} = 0.61$, and $\rho_{org} = 1\,g\,cm^{-3}$. Thus, a κ_{org} of 0 has to be assumed. To investigate the value of κ_{org} further, more sensitivity tests with the same values for κ_{sulf} and ρ_{org} were conducted only varying κ_{org} between 0 and 0.1 in steps of 0.01. The results are shown in Fig. 4. For the two lowest supersaturations, closure can be achieved within the uncertainties for various κ_{org} values between 0 and 0.1. However, taking the smallest difference as described before leads to a best fit for $\kappa_{org} = 0.02$, a slightly more hygroscopic value than assumed before. Closure can not be achieved with these conditions for 0.20% SS.

For the lowest three supersaturations, the results suggest that the measured organic compounds were not or only slightly soluble and that the ability of the particles to activate as CCN is dominated by the sulphate part of the particles. This might also be interpreted as particles analyzed by Leck and Bigg (2005a), which were internally mixed with an insoluble core.

These results contradict the findings of Lohmann and Leck (2005), who needed to invoke an activated Aitken mode with a surface-active fraction in a model study to be able to reproduce the number of measured CCN. This was especially observed for the ice camp station during the expedition AOE-96. Days with about similar meteorological conditions are encountered at the last days of the ASCOS study on the ice floe.

Consistent aerosol properties with our findings have been reported from the North Atlantic (Facchini et al., 2008). They found that the organic matter of submicron particles was almost entirely water insoluble and that the organic matter content increased with decreasing diameter of the particles. Furthermore, Ceburnis et al. (2008) presented a study of clean marine air at Mace Head, Ireland, where water insoluble organic carbon showed a net production at the surface in clean marine air, pointing to

ACPD
11, 8801–8840, 2011

a primary origin. This is consistent with our findings that the κ of the organic component is close to zero. However, one must keep in mind that these measurements were made over open ocean and are thus not directly comparable to our measurements. Flux measurements at an open lead carried out during the ASCOS campaign showed that particles coming from the sea surface cannot account for the total observed particle number variation in the surface mixing layer (Held et al., 2010). Hence, one might speculate that, as particles sources over the pack ice area seem to be weak, the measured slightly hygroscopic particles are transported from the open ocean water south of and along the ice edge. Note that the data from the open lead represents a point measurement whereas the sampling at the ship is an integrated measurement from all contributing sources.

The results are still ambiguous as the best values for κ_{org} and κ_{sulf} differ depending on the supersaturation. For 0.10% SS, closure could be achieved with $\kappa_{org} = 0, 0.1$, and 0.2. At this SS, only the largest particles (> 100 nm diameter) activate, for which diffusion losses are smallest and also the AMS measurements should be the most reliable. Therefore, 0.2 can be taken as an upper limit for κ_{org} based on our data.

The same permutations have also been applied for the analysis of the data from counter 2. The comparison of the 0.20% SS-data from the first counter and 0.22% SS-data from the second counter shows good agreement within the uncertainties (Fig. 5). Note that the actual supersaturation of counter 1 is not constant in time. The times at which the two counters measured at the considered supersaturations were also different, as counter 1 was changing its superaturation every 30 min and counter 2 started to measure at 0.22% SS only from 15 August onwards. However, the slope closest to 1 was again achieved with the same parameter settings, namely sensitivity permuation 13 (see Table 6).

As counter 2 was only measuring for four days on the ice floe with a supersaturation of 0.17%, the comparison with the 0.15% SS data from counter 1 is less significant, however, a linear fit from those data sets (counter 2 vs. counter 1) lead to a slope of 0.99.

Discussion Paper | Discussion Paper | Discussion Paper | Discussion Paper |

ACPD

11, 8801–8840, 2011

CCN Closure on Arctic Aerosol

M. Martin et al.

CCN_{pred}/CCN_{meas} against the time on the ice floe from the best fit (permutation 13) is shown in Fig. 6. The data is merged from the data of all five supersaturations from counter 1. During a rather long time period from DoY 233.9 to 238.1, many outliers are found at the two highest supersaturations. The calculated CCN numbers are mainly underpredicted there, assuming that the particles should be considered to be more hygroscopic to achieve closure. The κ value is varying between 0.1 and 0.4 over this time period. But again, since the AMS only measures particles larger than 70 nm in diameter, the small particles might have had a different composition then.

The time series of κ_{tot} from the best fit (permutation 13) is shown in Fig. 7. κ_{tot} exhibits a large variability, ranging from 0.09 to 0.61 (the latter value is reached when no organic mass at all was measured). The mean value over the entire campaign is 0.33 with a standard deviation (1-σ) of ± 0.13 which corresponds to about 50% of the mean value, making it not very representative of the hygroscopic properties for the total investigated time period. In a recent paper, Pringle et al. (2010) modelled the κ value globally and found an annual mean for the Arctic region of between 0.4 and 0.5. They used the ECHAM-MESSy Atmospheric Chemistry Model (EMAC) with seven aerosol classes (sulfate, black carbon, organic carbon, nitrate, ammonium, dust, sea salt) in several hydrophilic and hydrophobic modes and in the nucleation, Aitken, accumulation and coarse size range. For the time period while *Oden* was moored to the ice floe, this model gives a mean κ value of 0.26 ± 0.06, using the coordinates of the ship route (K. Pringle, personal communciation, 2010). This is a lower value than our measured one, but within its standard deviation.

Mean measured CCN number concentrations and standard deviations are shown in Table 3. As one can see, the mean concentrations are very low and also very variable. A more detailed study of CCN concerning different meteorological conditions will be carried out in a follow-up study. The importance of size-resolved chemistry for the CCN activity will be further studied by performing a CCN closure based on the hygroscopic growth as measured by a HTDMA.

ACPD
11, 8801–8840, 2011

6 Conclusions

An aerosol-cloud condensation nuclei (CCN) closure study based on observed CCN number concentration and physical and chemical submicrometer aerosol properties and concentrations was performed. The data shown here was collected during an expedition into the high Arctic (about 87° N) onboard an icebreaker during a three-week time period, when the ship was drifting passively moored to an ice floe. Measured CCN number concentrations at different supersaturations from two CCN counters were compared with predicted CCN number concentrations calculated from mass concentration data from an aerosol mass spectrometer and size distributions from a differential mobility particle sizer.

In general, closure was achieved within the measurement uncertainties for 0.10% supersaturation (SS), 0.15% and 0.20% SS from one counter, that scanned through five different supersaturations (counter 1), assuming an internally mixed aerosol and an insoluble or only slightly soluble organic volume fraction. For the two highest supersaturations, 0.41% SS and 0.73% SS, the predicted CCN numbers were overpredicted for all tested settings, in which the hygrosopicity, and the density of the organic fraction was varied, as well as the hygroscopicity of the sulfuric component, and 0% or 20% insoluble organic fraction was assumed. One way to explain this is by assuming that the smaller particles have a different composition than the larger ones, presumably an non-hygroscopic organic fraction.

Results from counter 1 at 0.10% SS give an upper limit of $\kappa_{org} = 0.2$, since the assumption of a more hygroscopic organic fraction results in overpredicted CCN concentrations. This means, that the organic fraction of the aerosols was nearly non-hygroscopic and does thus not contribute to droplet growth. The data from counter 1 at 0.20% SS compares well with that of counter 2, which was measuring at a constant supersaturation of 0.22%.

The assumptions concerning density and hygroscopicity could not be determined unambiguously, but the best constraints of $\kappa_{org} = 0.02, \kappa_{sulf} = 0.65$, and $\rho_{org} = 1\,g\,cm^{-3}$

ACPD
11, 8801–8840, 2011

lead to an overall mean κ value of 0.33 ± 0.13, with the variability in κ being rather large. κ showed a large variability throughout the experiment, suggesting that the hygroscopic properties of the aerosol changed during the campaign. The investigated data represents a CCN-mass closure for a time period of only three weeks, and as there are, to our knowledge, no similar high time resolved measurements of the high Arctic during its most biological active period into autumn freeze up conditions except for the more primitive CCN closures performed during previous Arctic expeditions, our results can thus not be compared in detail with other data.

For further investigations, the data will be compared with hygroscopicity data measured in the subsaturated regime. Moreover, different time periods will be investigated in more detail by case studies, i.e. taking meteorological conditions and time the air spent over the pack ice region into consideration.

Acknowledgements. This work is part of ASCOS (the Arctic Summer Cloud-Ocean Study). ASCOS was made possible by funding from the Knut and Alice Wallenberg Foundation and the DAMOCLES European Union 6th Framework Program Integrated Research Project. The Swedish Polar Research Secretariat (SPRS) provided access to the icebreaker Oden and logistical support. We are grateful to the SPRS logistical staff and to Oden's Captain Mattias Peterson and his crew. ASCOS is an IPY project under the AICIA-IPY umbrella and an endorsed SOLAS project. The authors would like to thank Douglas Orsini for providing the DMPS data and for useful discussions. The DMPS measurements were funded by the German Research Foundation No. HE939/29-1. The AMS measurements were supported by Arctic-SOLAS (Canada), Environment Canada, CFCAS (CAFC Network), NSERC (CGS D for RC), Richard Leaitch, Shao-Meng Li, Katherine Hayden and Dave Halpin. Additionally, we acknowledge financial support from the EU project EUCAARI (European Integrated project on Aerosol Cloud Climate and Air Quality interactions) No. 036833-2.

ACPD
11, 8801–8840, 2011

References

Andreae, M. O. and Rosenfeld, D.: Aerosol-cloud-precipitation interactions, Part 1, The nature and sources of cloud-active aerosols, Earth-Sci. Rev., 89, 13–41, doi:10.1016/j.earscirev.2008.03.001, 2008. 8814

Bigg, E. K. and Leck, C.: Cloud-active particles over the central Arctic Ocean, J. Geophys. Res., 106(D23), 32,155–32,166, 2001. 8805

Bigg, E. K., Leck, C., and Nilsson, E. D.: Sudden changes in arctic atmospheric aerosol concentrations during summer and autumn, Tellus 48B, 254–271, 1996. 8804

Bigg, E. K., Leck, C., and Nilsson, E. D.: Sudden Changes in Aerosol and Gas concentrations in the central Arctic Marine Boundary Layer – Causes and Consequences, J. Geophys. Res., 106(D23), 32,167–32,185, 2001. 8805

Birmili, W., Stratmann, F., and Wiedensohler, A.: Design of a DMA-based size s pectrometer for a large particle size range and stable operation, J. Aerosol Sci., 30(4), 549–553, 1999. 8811

Canagaratna, M. R., Jayne, J. T.,Jimenez, J. L., Allan, J. D., Alfarra, M. R., Zhang, Q., Onasch, T. B., Drewnick, F., Coe, H., Middlebrook, A. M., Delia, A. E., Williams, L. R., Trimborn, A. M., Northway, M. J., DeCarlo, P. F., Kolb, C. E., Davidovits, P., and Worsnop, D. R.: Chemical and microphysical characterization of ambient aerosols with the Aerodyne aerosol mass spectrometer, Mass Spec. Rev., 26, 185–222, 2007. 8810

Ceburnis, D., O'Dowd, C. D., Jennings, G. S., Facchini, M. C., Emblico, L., Decesari, S., Fuzzi, S., and Sakalys, J.: Marine aerosol chemistry gradients: Elucidating primary and secondary processes and fluxes, Geophys. Res. Lett., 35, L07804, doi:10.1029/2008GL033462, 2008. 8817

Chang, R. Y.-W., Abbatt, J. P.D. , Graus, M., Müller, M., Paatero, J., Hayden, K., Li, S.-M., Leaitch, W. R., Leck, C., and Tjernström, M.: Aerosol composition and sources in the central Arctic Ocean during ASCOS, Atmos. Chem. Phys., in preparation, 2010. 8810

Charlson, R. J., Lovelock, J. E., Andreae, M. O., and Warren, S. G.: Oceanic Phytoplankton, Atmospheric Sulfur, Cloud Albedo and Climate, Nature, 326, 655–661, 1987. 8804

Covert, D. S., Wiedensohler, A., Aalto, P. P., Heintzenberg, J., McMurry, P. H., and Leck, C.: Aerosol number size distributions from 3 to 500 nm diameter in the arctic marine boundary layer during summer and autumn, Tellus 48B, 197–212, 1996. 8804

Denman, K., Brasseur, G., Chidthaisong, A., Ciais, P., Cox, P., Dickinson, R., Hauglustaine, D., Heinze, C., Holland, E., Jacob, D., Lohmann, U., Ramachandran, S., Silva Dias, P., Wofsy, S., and Zhang, X.: Couplings between changes in the climate system and biogeochemistry, Climate Change 2007: The Physical Science Basis. Contribution of Working Group I to the Fourth Assessment Report of the Intergovernmental Panel on Climate Change, 499–588, edited by: Solomon, S., Qin, D., Manning, M., Chen, Z., Marquis, M., Averyt, K. B., Tignor, M., and Miller, H. L., Cambridge Univ. Press, Cambridge, United Kingdom and New York, NY, 2007. 8803

Drewnick, F., Hings, S. S., DeCarlo, P., Jayne, J. T., Gonin, M., Fuhrer, K., Weimer, S., Jimenez, J. L., Demerjian, K. L., Borrmann, S., and Worsnop, D. R.: A new time-of-flight aerosol mass spectrometer (TOF-AMS) – Instrument description and first field deployment, Aerosol Sci. Technol., 39(7), 637–658, 2005. 8810

Facchini, M. C., Rinaldi, M., Decesari, S., Carbone, C., Finessi, E., Mircea, M., Fuzzi, S., Ceburnis, D., Flanagan, R., Nilsson, E. D., de Leeuw, G., Martino, M., Woeltjen, J., and O'Dowd, C. D.: Primary submicron marine aerosol dominated by insoluble organic colloids and aggregates, Geophys. Res. Lett., 35, L17814, doi:10.1029/2008GL034210, 2008. 8817

Heintzenberg, J., and Leck, C.: Seasonal variations of the atmospheric aerosol near the top of the marine boundary layer over Spitsbergen related to the Arctic sulfur cycle, Tellus 46B, 52–67, 1994. 8803, 8804

Heintzenberg, J., Leck, C., Birmili, W., Wehner, B., Tjernström, M., and Wiedensohler A.: Aerosol number-size distributions during clear and fog periods in the summer high Arctic: 1991, 1996 and 2001, Tellus B, 58, 41–50, doi:10.1111/j.1600-0889.2005.00171.x, 2006. 8804

Held, A., Brooks, I. M., Leck, C., and Tjernström, M.: On the potential contribution of open lead particle emissions to the central Arctic aerosol concentration, Atmos. Chem. Phys. Disc., 10, 24961–24992, doi:10.5194/acpd-10-24961-2010, 2010. 8818

Intrieri, J. M., Shupe, M. D., Uttal, T., and McCarty, B. J.: An annual cycle of Arctic cloud characteristics observed by radar and lidar at SHEBA, J. Geophys. Res., 107(C10), 8030, doi:10.1029/2000JC000423, 2002. 8803

Jimenez, J. L., Jayne, J. T., Shi, Q., Kolb, C. E., Worsnop, D. R., Yourshaw, I., Seinfeld, J. H., Flagan, R. C., Zhang, X., Smith, K. A., Morris, J. W., and Davidovits, P.: Ambient aerosol sampling using the Aerodyne Aerosol Mass Spectrometer, J. Geophys. Res., 108(D7), 8425, doi:10.1029/2001JD001213, 2003. 8810

Kammermann, L., Gysel, M., Weingartner, E., Herich, H., Cziczo, D. J., Holst, T., Svennings-

ACPD
11, 8801–8840, 2011

Title Page
Abstract | Introduction
Conclusions | References
Tables | Figures
◀| |▶
◀ ▶
Back | Close
Full Screen / Esc
Printer-friendly Version
Interactive Discussion

son, B., Arneth, A., and Baltensperger, U.: Subarctic atmospheric aerosol composition: 3. Measured and modeled properties of cloud condensation nuclei, J. Geophys. Res., 115, D04202, doi:10.1029/2009JD012447, 2010. 8814

Kay, J. E., and Gettelman, A.: Cloud influence on and response to seasonal Arctic sea ice loss, J. Geophys. Res., 114, D18204, doi:10.1029/2009JD011773, 2009. 8803

Korhonen, H., Carslaw, K. S., Spracklen, D. V., Ridley, D. A., and Strom, J.: A global model study of processes controlling aerosol size distributions in the Arctic spring and summer, J. Geophys. Res., 113, D08211, doi:10.1029/2007JD009114, 2008. 8803

Lannefors, H., Heintzenberg, J., and Hansson, H. C.: A comprehensive study of physical and chemical parameters of the Arctic summer aerosol; results from the Swedish expedition Ymer-80, Tellus, 35B, 40–54, 1983. 8805

Leck, C. and Bigg, E. K.: Biogenic particles in the surface microlayer and overlaying atmosphere in the central Artic ocean during summer, Tellus, 57B, 305, 305–316, 2005a. 8804, 8817

Leck, C. and Bigg, E. K.: Source and evolution of the marine aerosol – a new perspective, Geophys. Res. Lett., 32, L19803, doi:10.1029/2005GL023651, 2005b. 8804

Leck, C. and Persson, C.: The central Arctic Ocean as a source of dimethyl sulfide-Seasonal variability in relation to biological activity, Tellus B, 48(2), 156–177, 1996. 8804

Leck, C., Bigg, E. K., Covert, D. S., Heintzenberg, J., Maenhaut, W., Nilsson, E. D., and Wiedensohler, A.: Overview of the Atmospheric research program during the International Arctic Ocean Expedition 1991 (IAOE-91) and its scientific results, Tellus, 48B, 136–155, 1996. 8804

Leck, C., Nilsson, E. D., Bigg, E. K., and Bäcklin, L.: Atmospheric program on the Arctic Ocean Expedition 1996 (AOE-96): An overview of scientific goals, experimental approach, and instruments, J. Geophys. Res., 106, 32051–32067, 2001. 8804, 8807

Leck, C., Norman, M., Bigg, E. K., and Hillamo, R.: Chemical composition and sources of the high Arctic aerosol relevant for fog and cloud formation, J. Geophys. Res., 107(D12), doi:10.1029/2001JD001463, 4135, 2002. 8805

Leck, C., Tjernström, M., Matrai, P., Swietlicki, E., and Bigg, E. K.: Can Marine Micro-organisms Influence Melting of the Arctic Pack Ice?, Eos, 85, 3, 25–36, 2004. 8804

Li, S. M., and Barrie, L. A.: Biogenic sulphur aerosol in the Arctic troposphere: 1. Contributions to total sulfate, J. Geophys. Res., 98, 20613–20622, 1993. 8804

Lohmann, U. and Feichter, J.: Global indirect aerosol effects: a review, Atmos. Chem. Phys.

ACPD
11, 8801–8840, 2011

CCN Closure on Arctic Aerosol

M. Martin et al.

Discuss., 4, 7561–7614, doi:10.5194/acpd-4-7561-2004, 2004. 8803

Lohmann, U. and Leck, C.: Importance of submicron surface-active organic aerosols for pristine Arctic clouds, Tellus B, 57(3), 261–268, 2005. 8817

Mauritsen, T., Sedlar, J., Tjernström, M., Leck, C., Martin, M., Shupe, M., Sjogren, S., Sierau, B., Persson, P. O. G., Brooks, I. M., and Swietlicki, E.: An Arctic CCN-limited cloud-aerosol regime, Atmos. Chem. Phys., 11, 165–173, doi:10.5194/acp-11-165-2011, 2011. 8805

Muhlbauer, A., Spichtinger, P., and Lohmann, U.: Application and Comparison of Robust Linear Regression Methods for Trend Estimation, J. Appl. Meteor. Climatol., 48(9), 1961–1970, 2009. 8815

Nilsson, E. D., and Leck, C.: A pseudo-Lagrangian study of the arctic remote marine sulfur cycle, Tellus, 54B, 213–230, 2002. 8804

Paatero, J., Vaattovaara, P., Vestenius, M., Meinander, O., Makkonen, U., Kivi, R., Hyvärinen, A., Asmi, E., Tjernström, M., and Leck, C.: Finnish contribution to the Arctic Summer Cloud Ocean Study (ASCOS) expedition, Arctic Ocean 2008, Geophysica, 45(1–2), 119–146, 2009. 8807

Petters, M. D. and Kreidenweis, S. M.: A single parameter representation of hygroscopic growth and cloud condensation nucleus activity, Atmos. Chem. Phys., 7, 1961–1971, doi:10.5194/acp-7-1961-2007, 2007. 8806, 8813, 8814

Pringle, K. J., Tost, H., Pozzer, A., Pöschl, U., and Lelieveld, J.: Global distribution of the effective aerosol hygroscopicity parameter for CCN activation, Atmos. Chem. Phys., 10, 5241–5255, doi:10.5194/acp-10-5241-2010, 2010. 8819

Quinn, P. K., Miller, T. L., Bates, T. S., Ogren, J. A., Andrews, E., and Shaw, G. E.: A three-year record of simultaneously measured aerosol chemical and optical properties at Barrow, Alaska, J. Geophys. Res., 107(D11), 4130, doi:10.1029/2001JD001248, 2002. 8804

Roberts, G. C. and Nenes, A.: A Continuous-Flow Streamwise Thermal-Gradient CCN Chamber for Atmospheric Measurements, Aerosol Sci. Technol., 39(3), 206–221, doi:10.1080/027868290913988, 2005. 8808

Rose, D., Gunthe, S. S., Mikhailov, E., Frank, G. P., Dusek, U., Andreae, M. O., and Pöschl, U.: Calibration and measurement uncertainties of a continuous-flow cloud condensation nuclei counter (DMT-CCNC): CCN activation of ammonium sulfate and sodium chloride aerosol particles in theory and experiment, Atmos. Chem. Phys., 8, 1153–1179, doi:10.5194/acp-8-1153-2008, 2008. 8809

Rousseeuw, P. J.: Least Median of Squares Regression, J. Amer. Stat. Assoc., 79(388), 871–

ACPD
11, 8801–8840, 2011

880, 1984. 8815
Rousseeuw, P. J. and Van Driessen, K.: Computing LTS Regression for Large Data Sets, Data Min. Knowl. Disc., 12, 29–45, 2006. 8815
Sedlar, J., Tjernström, M., Mauritsen, T., Shupe, M., Brooks, I., Persson, P., Birch, C., Leck, C., Sirevaag, A., and Nicolaus, M.: A transitioning Arctic surface energy budget: the impacts of solar zenith angle, surface albedo and cloud radiative forcing, Clim. Dyn., 1–18, 2010. 8803
Seinfeld, J. H. and Pandis, S. N.: Atmospheric Chemistry and Physics: From Air Pollution to Climate Change, New York, John Wiley & Sons, Inc., USA, 1998. 8812
Shaw, G. E.: The Arctic Haze Phenomenon, Bull. Amer. Meteor. Soc., 76(12), 2403–2413, 1995. 8803
Stohl, A., Andrews, E., Burkhart, J. F., Forster, C., Herber, A., Hoch, S. W., Kowal, D., Lunder, C., Mefford, T., Ogren, J. A., Sharma, S., Spichtinger, N., Stebel, K., Stone, R., Strom, J., Torseth, K., Wehrli, C., and Yttri, K. E.: Pan-Arctic enhancements of light absorbing aerosol concentrations due to North American boreal forest fires during summer 2004, J. Geophys. Res., 111, D22214, doi:10.1029/2006JD007216, 2006. 8804
Tjernström, M., Sedlar, J., and Shupe, M.: How well do regional climate models reproduce radiation and clouds in the Arctic? An evaluation of ARCMIP simulations, J. Clim. Appl. Meteorol., 47, 2405–2422, 2008. 8803
Twomey, S. A.: The influence of pollution on the shortwave albedo of clouds, J. Atmos. Sci., 34, 1149–1152, 1977. 8803
Walsh, J., Kattsov, V., Chapman, W., Govorkova, V., and Pavlova, T.: Comparison of Arctic climate simulations by uncoupled and coupled global models, J. Climate, 15(12), 1429–1446, 2002. 8803
Zhou, J., Swietlicki, E., Berg, O. H., Aalto, P. P., Hämeri, K., Nilsson, E. D., and Leck, C.: Hygroscopic properties of aerosol particles over the central Arctic Ocean during summer, J. Geophys. Res., 106(D23), 32111–32123, doi:10.1029/2000JD900426, 2001. 8805

ACPD
11, 8801–8840, 2011

CCN Closure on Arctic Aerosol

M. Martin et al.

Table 1. The different measured supersaturations throughout the study. For simplicity, the mean values from counter 1 are used. All closure calculations were done using the respective mean supersaturation for each point in time.

	Time Period	SS 1 [%]	SS 2 [%]	SS 3 [%]	SS 4 [%]	SS5 [%]
Counter 1	07/08–10/08	0.089 ± 0.006	0.161 ± 0.009	0.233 ± 0.013	0.521 ± 0.045	0.952 ± 0.094
	10/08–12/08	0.082 ± 0.006	0.126 ± 0.007	0.171 ± 0.009	0.347 ± 0.026	0.613 ± 0.056
	12/08–21/08	0.102 ± 0.007	0.146 ± 0.008	0.189 ± 0.010	0.362 ± 0.028	0.622 ± 0.058
	21/08–08/09	0.106 ± 0.007	0.158 ± 0.009	0.210 ± 0.010	0.416 ± 0.034	0.725 ± 0.069
mean values		0.10	0.15	0.20	0.41	0.73
Counter 2	04/08–15/08		0.170 ± 0.010			
	15/08-08/09			0.219 ± 0.009		

ACPD
11, 8801–8840, 2011
CCN Closure on Arctic Aerosol
M. Martin et al.

Table 2. Table with the different parameter values for the performed closure studies. For a detailed listing of the different permutations, see Appendix Table.

Parameters	Description	investigated values
κ_{org}		0,0.1,0.2,0.3,0.4
κ_{sulf}		0.61,0.65,0.7
ρ_{org}	[g cm^{-3}]	1,1.2,1.6
insoluble organic fraction		0%, 20%

ACPD
11, 8801–8840, 2011

Table 3. The mean CCN concentrations and standard deviations for all five measured supersaturations of counter 1, averaged over the time period of the ice drift.

Supersaturation (%)	mean CCN concentration ($1\,cm^{-3}$)	standard deviation
0.10	14.01	10.96
0.15	19.96	15.15
0.20	26.55	19.63
0.41	34.62	22.67
0.73	46.99	37.43

ACPD
11, 8801–8840, 2011

Table A1. Table with the different parameter settings for the performed closure studies.

number	κ_{org}	κ_{sulf}	ρ_{org} [$g\,cm^{-3}$]	ρ_{ins} [$g\,cm^{-3}$]
1	0	0.7	1	1
2	0	0.7	1	0
3	0	0.7	1.2	1
4	0	0.7	1.2	0
5	0	0.7	1.6	1
6	0	0.7	1.6	0
7	0	0.65	1	1
8	0	0.65	1	0
9	0	0.65	1.2	1
10	0	0.65	1.2	0
11	0	0.65	1.6	1
12	0	0.65	1.6	0
13	0	0.61	1	1
14	0	0.61	1	0
15	0	0.61	1.2	1
16	0	0.61	1.2	0
17	0	0.61	1.6	1
18	0	0.61	1.6	0
19	0.1	0.7	1	1
20	0.1	0.7	1	0
21	0.1	0.7	1.2	1
22	0.1	0.7	1.2	0
23	0.1	0.7	1.6	1

ACPD
11, 8801–8840, 2011

Table A1. Continued.

number	κ_{org}	κ_{sulf}	ρ_{org} [$g\,cm^{-3}$]	ρ_{ins} [$g\,cm^{-3}$]
24	0.1	0.7	1.6	0
25	0.1	0.65	1	1
26	0.1	0.65	1	0
27	0.1	0.65	1.2	1
28	0.1	0.65	1.2	0
29	0.1	0.65	1.6	1
30	0.1	0.65	1.6	0
31	0.1	0.61	1	1
32	0.1	0.61	1	0
33	0.1	0.61	1.2	1
34	0.1	0.61	1.2	0
35	0.1	0.61	1.6	1
36	0.1	0.61	1.6	0
37	0.2	0.7	1	1
38	0.2	0.7	1	0
39	0.2	0.7	1.2	1
40	0.2	0.7	1.2	0
41	0.2	0.7	1.6	1
42	0.2	0.7	1.6	0
43	0.2	0.65	1	1
44	0.2	0.65	1	0
45	0.2	0.65	1.2	1
46	0.2	0.65	1.2	0

ACPD
11, 8801–8840, 2011

Table A1. Continued.

number	κ_{org}	κ_{sulf}	ρ_{org} [g cm^{-3}]	ρ_{ins} [g cm^{-3}]
47	0.2	0.65	1.6	1
48	0.2	0.65	1.6	0
49	0.2	0.61	1	1
50	0.2	0.61	1	0
51	0.2	0.61	1.2	1
52	0.2	0.61	1.2	0
53	0.2	0.61	1.6	1
54	0.2	0.61	1.6	0
55	0.3	0.7	1	1
56	0.3	0.7	1	0
57	0.3	0.7	1.2	1
58	0.3	0.7	1.2	0
59	0.3	0.7	1.6	1
60	0.3	0.7	1.6	0
61	0.3	0.65	1	1
62	0.3	0.65	1	0
63	0.3	0.65	1.2	1
64	0.3	0.65	1.2	0
65	0.3	0.65	1.6	1
66	0.3	0.65	1.6	0
67	0.3	0.61	1	1
68	0.3	0.61	1	0

ACPD
11, 8801–8840, 2011

Table A1. Continued.

number	κ_{org}	κ_{sulf}	ρ_{org} [g cm^{-3}]	ρ_{ins} [g cm^{-3}]
69	0.3	0.61	1.2	1
70	0.3	0.61	1.2	0
71	0.3	0.61	1.6	1
72	0.3	0.61	1.6	0
73	0.4	0.7	1	1
74	0.4	0.7	1	0
75	0.4	0.7	1.2	1
76	0.4	0.7	1.2	0
77	0.4	0.7	1.6	1
78	0.4	0.7	1.6	0
79	0.4	0.65	1	1
80	0.4	0.65	1	0
81	0.4	0.65	1.2	1
82	0.4	0.65	1.2	0
83	0.4	0.65	1.6	1
84	0.4	0.65	1.6	0
85	0.4	0.61	1	1
86	0.4	0.61	1	0
87	0.4	0.61	1.2	1
88	0.4	0.61	1.2	0
89	0.4	0.61	1.6	1
90	0.4	0.61	1.6	0

ACPD
11, 8801–8840, 2011

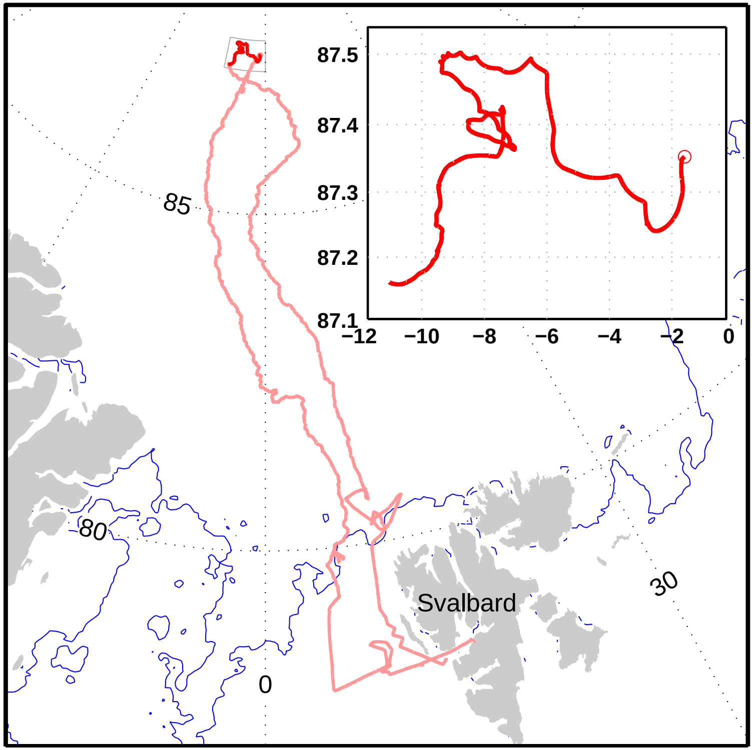

Fig. 1. The cruise route of *Oden*, enlarged is the time of the drift with the ice floe.

ACPD
11, 8801–8840, 2011

CCN Closure on Arctic Aerosol

M. Martin et al.

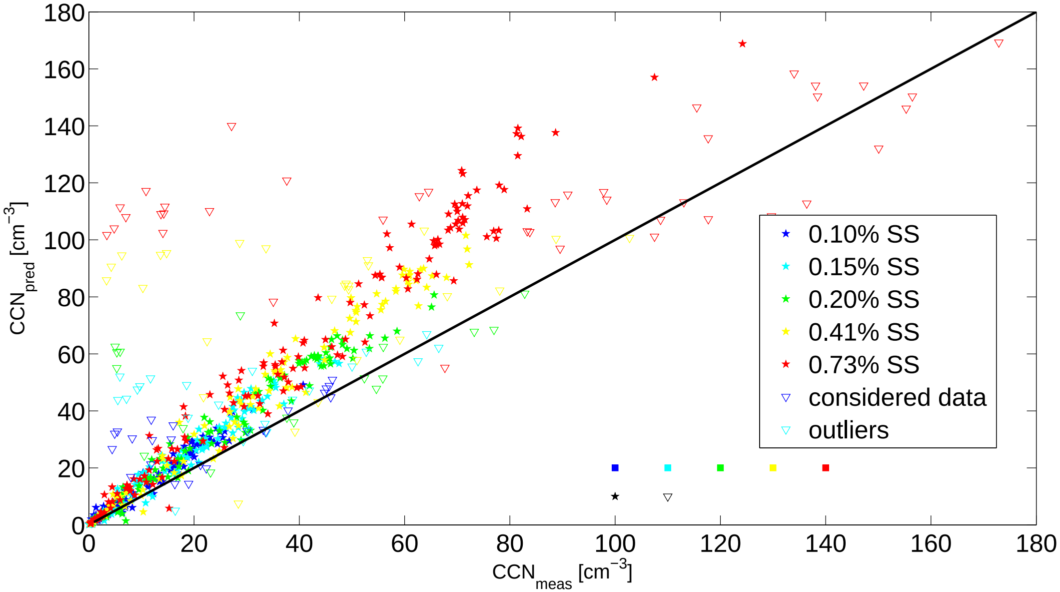

Fig. 2. Sample result of the closure study for permutation 62 ($\kappa_{org} = 0.3$, $\kappa_{sulf} = 0.65, \rho_{org} = 1\,g\,cm^{-3}$, no insoluble organic fraction assumed). The closure is overpredicted for all five supersaturations.

ACPD
11, 8801–8840, 2011

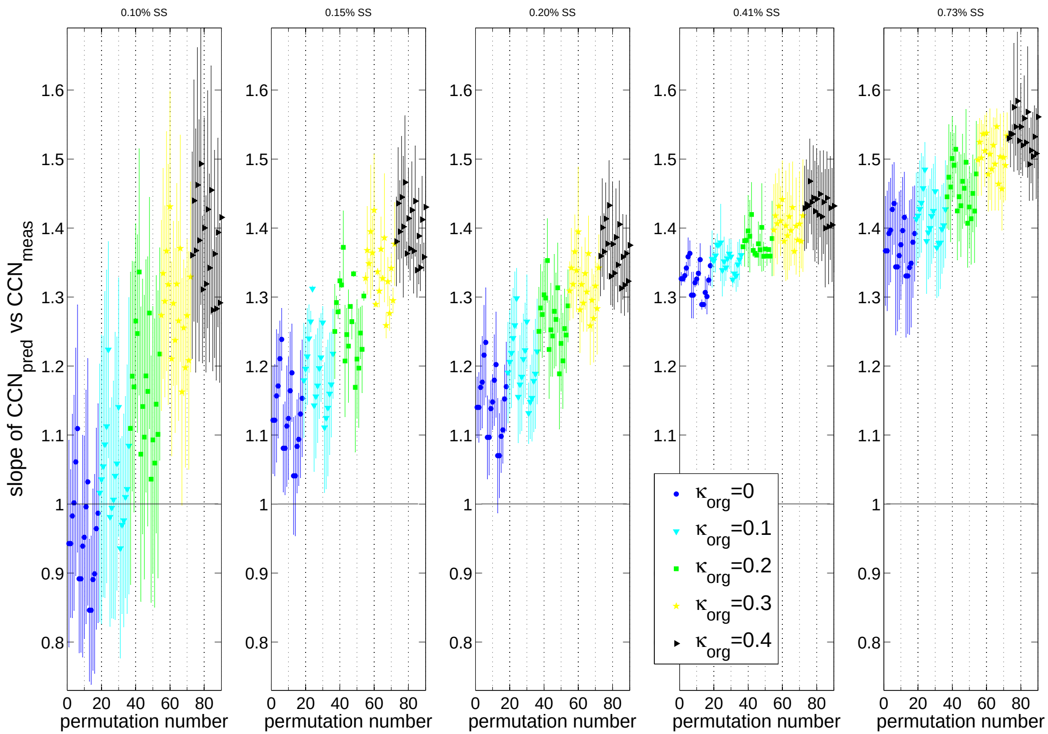

Fig. 3. The fitted slope of CCN_{pred} vs. CCN_{meas} for the different permuted assumptions and each supersaturation.

ACPD
11, 8801–8840, 2011

CCN Closure on Arctic Aerosol

M. Martin et al.

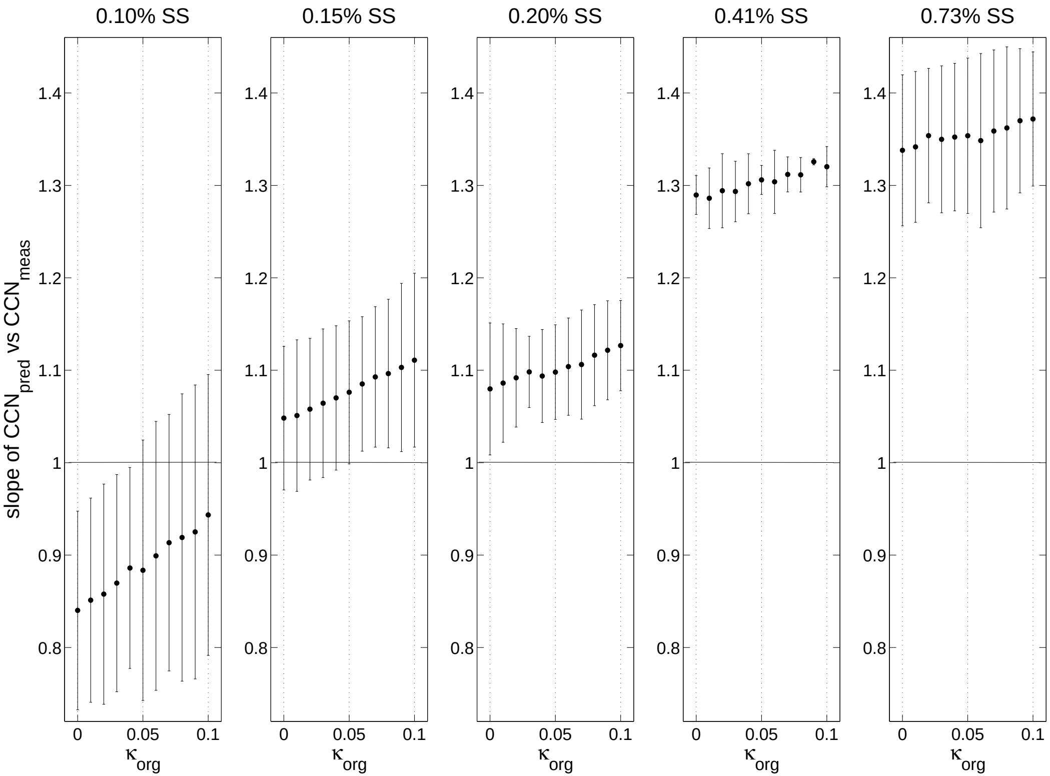

Fig. 4. The slope of CCN_{pred} vs CCN_{meas} for permutation 13 ($\kappa_{sulf} = 0.61, \rho_{org} = 1\,g\,cm^{-3}$), varying κ_{org} between 0 and 0.1.

ACPD
11, 8801–8840, 2011

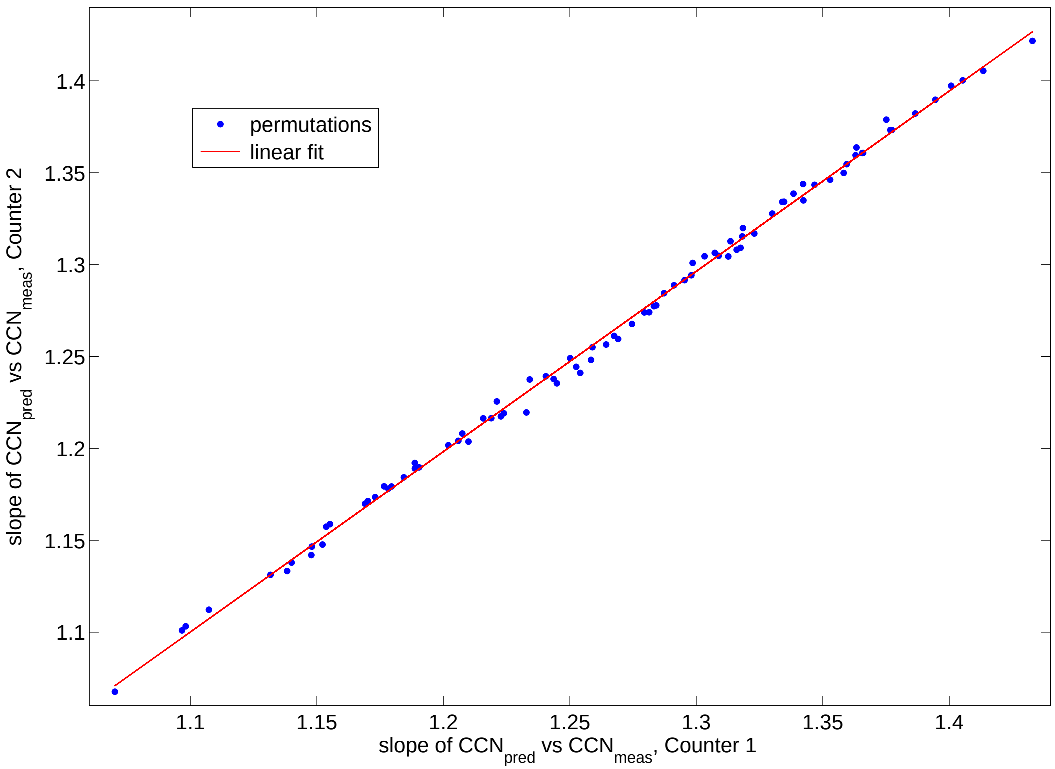

Fig. 5. The comparison of the permutation results of the first and the second CCN counter for 0.20% SS and 0.22% SS, respectively. The slope of the linear fit was 0.98, thus represents a very good correlation.

ACPD
11, 8801–8840, 2011

CCN Closure on Arctic Aerosol

M. Martin et al.

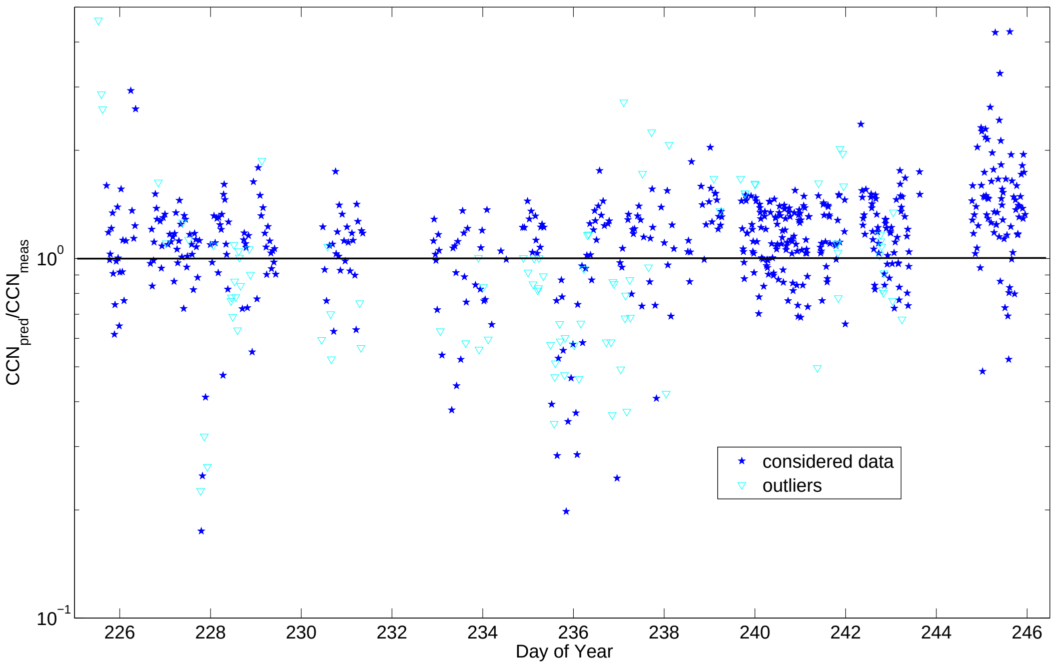

Fig. 6. Time series of CCN_{pred}/CCN_{meas} for all five supersaturation using the parameters of permutation 13 ($\kappa_{org} = 0.0$, $\kappa_{sulf} = 0.61$, $\rho_{org} = 1\,g\,cm^{-3}$).

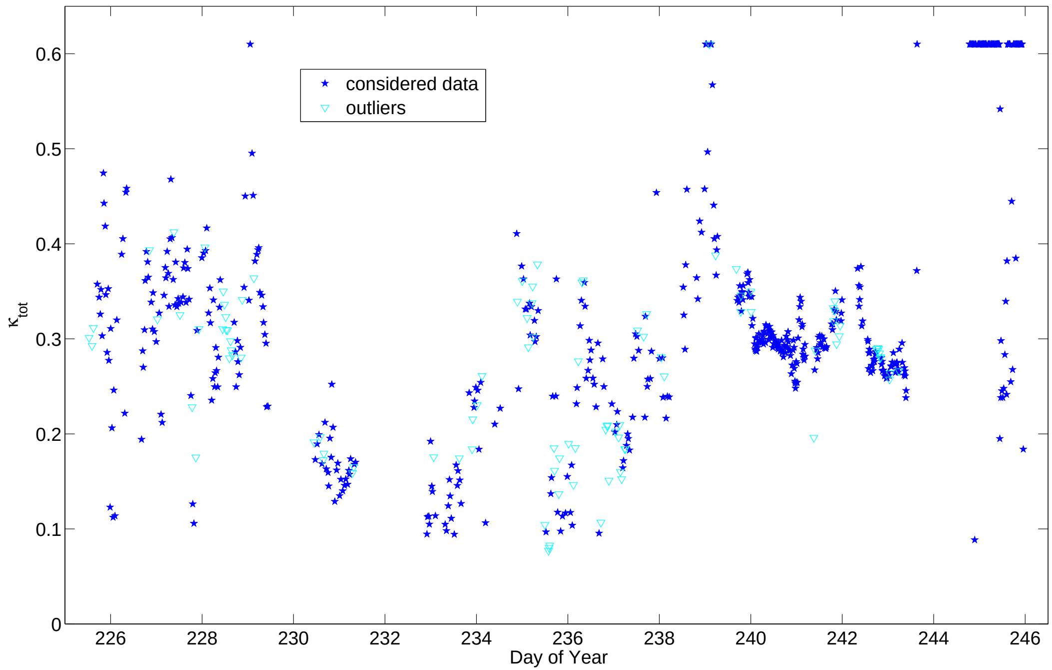

Fig. 7. The time series of the total κ value using the parameters of permutation 13 ($\kappa_{org} = 0.0$, $\kappa_{sulf} = 0.61$, $\rho_{org} = 1\,\mathrm{g\,cm^{-3}}$).

ACPD
11, 8801–8840, 2011